Lale Ozcan,[1] Xiaoming Xu,[1] Shi-Xian Deng,[1] Devram S. Ghorpade,[1] Tiffany Thomas,[2,3] Serge Cremers,[1,2,3] Brian Hubbard,[4] Michael H. Serrano-Wu,[4] Matthias Gaestel,[5] Donald W. Landry,[1] and Ira Tabas[1,2,6]

Treatment of Obese Insulin-Resistant Mice With an Allosteric MAPKAPK2/3 Inhibitor Lowers Blood Glucose and Improves Insulin Sensitivity

Diabetes 2015;64:3396–3405 | DOI: 10.2337/db14-1945

The prevalence of obesity-induced type 2 diabetes (T2D) is increasing worldwide, and new treatment strategies are needed. We recently discovered that obesity activates a previously unknown pathway that promotes both excessive hepatic glucose production (HGP) and defective insulin signaling in hepatocytes, leading to exacerbation of hyperglycemia and insulin resistance in obesity. At the hub of this new pathway is a kinase cascade involving calcium/calmodulin-dependent protein kinase II (CaMKII), p38α mitogen-activated protein kinase (MAPK), and MAPKAPK2/3 (MK2/3). Genetic-based inhibition of these kinases improves metabolism in obese mice. Here, we report that treatment of obese insulin-resistant mice with an allosteric MK2/3 inhibitor, compound (cmpd) 28, ameliorates glucose homeostasis by suppressing excessive HGP and enhancing insulin signaling. The metabolic improvement seen with cmpd 28 is additive with the leading T2D drug, metformin, but it is not additive with dominant-negative MK2, suggesting an on-target mechanism of action. Allosteric MK2/3 inhibitors represent a potentially new approach to T2D that is highly mechanism based, has links to human T2D, and is predicted to avoid certain adverse effects seen with current T2D drugs.

Type 2 diabetes (T2D) and its complications constitute an enormous public health problem worldwide and are an important cause of morbidity and mortality in modern society. Despite significant progress in our understanding of the pathophysiology of T2D, its incidence and prevalence continue to increase in epidemic proportions (1). Thus, new approaches are needed to contain this pandemic. Because T2D is a progressive disease, current treatment options are limited, and there is a need for combination therapy to improve long-term glycemic control. Excessive hepatic glucose production (HGP) is a key defect found in T2D (2), and it is driven in large part by chronic hyperglucagonemia coupled with insufficient hepatic insulin action (3,4). Moreover, through excess nutrient intake and perturbations in endoplasmic reticulum (ER) calcium, obesity induces ER stress in both preclinical models of T2D and humans, and this leads to perturbations in insulin signaling (5–8). However, therapeutic translation of these findings has been difficult. Drugs that antagonize glucagon action potently lower blood glucose and HbA_{1c} in humans with T2D, but adverse effects on plasma lipids have limited their development (9–11). So-called chemical chaperones can relieve ER stress and diabetes in obese mice, but their mechanism of action is not well understood, limiting their therapeutic translation (12).

We recently reported that excessive glucagon signaling in obesity activates a kinase cascade in hepatocytes (HCs) that, via two separate downstream signaling branches, promotes increased HGP and, through ER stress, defective insulin signaling (13,14) (Supplementary Fig. 1). This pathway, therefore, links obesity to the two cardinal features of T2D: hyperglycemia and selective insulin resistance. The kinases include calcium/calmodulin-dependent protein kinase II (CaMKII), p38α mitogen-activated protein kinase

[1]Department of Medicine, Columbia University, New York, NY
[2]Department of Pathology and Cell Biology, Columbia University, New York, NY
[3]Irving Institute for Clinical and Translational Research, Columbia University, New York, NY
[4]Tabomedex Biosciences, Boxford, MA
[5]Department of Biochemistry, Hannover Medical School, Hannover, Germany
[6]Department of Physiology and Cellular Biophysics, Columbia University, New York, NY

Corresponding authors: Lale Ozcan, lo2192@columbia.edu, and Ira Tabas, iat1@columbia.edu.

Received 29 December 2014 and accepted 4 June 2015.

This article contains Supplementary Data online at http://diabetes.diabetesjournals.org/lookup/suppl/doi:10.2337/db14-1945/-/DC1.

(MAPK), and MAPKAPK2 (MK2) and the highly homologous MAPKAPK3 (MK3), which are downstream targets of p38α. The pathway is activated in the livers of both hyperphagic and diet-induced models of obesity. Our evidence to date suggests that CaMKII-activated p38α MAPK is the kinase responsible for the downstream effects leading to metabolic disturbance in obesity (13,14) (L.O., I.T., unpublished data). Nonetheless, genetic inhibition of any kinases in obese mice markedly improves blood glucose and insulin resistance, because CaMKII is upstream of p38, and MK2/3 inhibition destabilizes and thereby suppresses p38 activity (15,16). The molecular mechanistic underpinnings of these in vivo results could be recapitulated in studies using primary HCs from both mice and humans (13,14).

The discovery of this new pathway suggested that it may be a novel therapeutic target for the treatment of T2D. We focused on the common kinase hub so that both excessive HGP and defective insulin signaling could be treated. However, direct p38 inhibitors have adverse effects when tested in animal models (15,17,18), and while CaMKII inhibitors are a theoretical target option, the only CaMKII inhibitors published to date are ATP competitive, which limits their specificity. We therefore turned our attention to MK2/3 because highly specific non–ATP-competitive ("allosteric") MK2/3 inhibitors have been developed recently, including a potent inhibitor called compound (cmpd) 28 (19) and MK2/3 inhibition suppresses p38 activity in a manner that avoids the adverse effects of direct p38 inhibition (15,16). Here, we show that treatment of obese mice with cmpd 28 leads to a significant improvement in glucose metabolism via a mechanism that is consistent with inhibition of the aforementioned biochemical pathway. Importantly, this improvement is additive with metformin, one of the most effective therapeutics for treating T2D. Collectively, these results help validate MK2/3 as a therapeutic target and MK2/3 inhibitors as treatment for obesity-associated T2D.

RESEARCH DESIGN AND METHODS

Reagents and Antibodies

Forskolin, tumor necrosis factor α, and metformin were from Sigma. Anti–phospho-Akt, anti-Akt, anti–phospho-hsp25, anti-hsp25, anti-FoxO1, and anti-nucleophosmin antibodies were from Cell Signaling; anti-Trb3 was from Millipore; and anti–β-actin antibody was from Abcam. Adeno–T222A-MK2 was purchased from Cell Biolabs, Inc. Cmpd 28 was synthesized according to the synthetic route reported by Huang et al. (19). Briefly, commercially available 5-(4-cyanophenyl) furan-2-carboxylic acid and tert-butyl 4-(4-aminophenyl) piperazine-1-carboxylate were coupled with EDC and HOBt to provide the corresponding amide in quantitative yield. The alkylation of the amide with 2-bromobenzyl bromide under basic conditions gave the *N*-alkylated product in 96% yield. Suzuki coupling of the resulting compound with 4-methoxy-3-pyridine boronic acid gave the coupling product in 63% yield. Deprotection of the Boc protecting group with trifluoroacetic acid (TFA) provided the TFA salt of cmpd 28. The resulting TFA salt was converted to the HCl salt by adding 2 mol/L HCl in ether followed by solvent evaporation. All of the compounds were purified by column chromatography and characterized by nuclear magnetic resonance and liquid chromatography–mass spectrometry. The final product, cmpd 28, showed a purity of >98% by LC/MS analysis.

Mouse Experiments

$Mk2^{-/-}Mk3^{+/-}$ mice were created as described previously (20). *ob/ob* mice were obtained from The Jackson Laboratory. For diet-induced obese (DIO) mice studies, wild-type (WT) male mice were fed a high-fat diet with 60% kcal from fat (Research Diets) and maintained on a 12-h light-dark cycle. Recombinant adenovirus ($0.5–3 \times 10^9$ plaque-forming units/mouse) was delivered by tail vein injection, and experiments were commenced after 5–7 days. Mice were treated by daily intraperitoneal (i.p.) injections of 0.2 mg/kg body wt cmpd 28 in sterile water, 200 mg/kg body wt metformin in sterile PBS, or water or PBS vehicle control (between 8:00 A.M. and 10:00 A.M.). Fasting blood glucose was measured in mice that were fasted for 4–6 h, with free access to water, using a glucose meter. Glucose tolerance tests were performed in overnight-fasted mice by assaying blood glucose at various times after injection of glucose (0.5 g/kg body wt i.p. for *ob/ob*). Plasma insulin levels were measured using an ultra-sensitive mouse insulin ELISA kit (Crystal Chem). Insulin tolerance tests were performed in 5-h-fasted mice by assaying blood glucose at various times after injection of insulin (2 IU/kg body wt i.p. for *ob/ob*). Pyruvate tolerance tests were carried out with an injection of 2 g/kg body wt i.p. pyruvate after 17 h of fasting. Blood glucose levels were measured over the next 2 h. For determination of the plasma and liver distribution of cmpd 28, blood and liver tissues samples were collected from individual *ob/ob* mice at 5, 15, 30, 60, and 120 min after injection of cmpd 28 at a dose of 0.2 mg/kg body wt i.p. (n = 3 mice per group). Plasma and liver homogenates were extracted with acetonitrile/methanol (4:1), resolubilized with 25% methanol, and injected onto an Agilent Poroshell 120 EC-C18 column linked to an Agilent 1290 Infinity UHPLC running at 45°C at 0.5 mL/min. Cmpd 28 was detected with an Agilent 6410 tandem mass spectrometer with positive electrospray ionization monitoring the +H quantifying ion transition 570.2 to 330.2 (collision energy = 45 V; Fragmentor = 210 V) and qualifying ion transition 570.2 to 196 (collision energy = 81 V; Fragmentor = 210 V). Plasma that was spiked with known concentrations of cmpd 28 was used to create a standard curve, which was linear from 10 ng/mL to 100 ng/mL. The MS conditions were as follows: gas temperature = 300°C, gas flow = 13 L/min, nebulizer = 60 ψ, and capillary = 3,000 V. Animal studies were performed in accordance with the Columbia University Institutional Animal Care and Use Committee.

Portal Vein Insulin Infusion and Protein Extraction From Tissues

After 5 h food withdrawal, mice were anesthetized, and insulin (1 IU/kg body wt for DIO and 2 IU/kg body wt for *ob/ob*) or PBS was injected into mice through the portal vein. Three-to-four minutes after injection, tissues were removed, frozen in liquid nitrogen, and kept at −80°C until processing. For protein extraction, tissues were placed in a cold lysis buffer (25 mmol/L Tris-HCl pH 7.4, 1 mmol/L EGTA, 1 mmol/L EDTA, 10 mmol/L $Na_4P_2O_7$, 10 mmol/L NaF, 2 mmol/L Na_3VO_4, 1% NP-40, 2 mmol/L phenylmethylsulfonyl fluoride, 5 μg/mL leupeptin, 10 nmol/L okadaic acid, and 5 μg/mL aprotinin). After homogenization on ice, the tissue lysates were centrifuged, and the supernatant fractions were used for immunoblot analysis.

Primary HCs

Primary mouse HCs were isolated from 8- to 12-week-old mice as described previously (13). For most experiments, the HCs were cultured in DMEM containing 10% FBS, treated as described in the figure legends, and then incubated for 5 h in serum-free DMEM.

Glucose Production in Primary HCs

Glucose production assays were carried out as previously described (13). Briefly, after primary mouse HCs were harvested and cultured as described above, the cell culture medium was switched to glucose- and phenol-free DMEM (pH 7.4) supplemented with 20 mmol/L sodium lactate, 2 mmol/L sodium pyruvate, and 10 μm forskolin. After incubation for the designated times, 100 μL medium was collected, and the glucose content was measured using a colorimetric glucose assay kit (Abcam). The data were normalized to the total protein amount in the whole-cell lysates.

Immunostaining

The pancreas was harvested from the mice at the time of sacrifice and fixed in 10% neutral-buffered formalin for 24 h and then embedded in paraffin. Sections (5 μm) were incubated overnight with rabbit anti-glucagon (1:200; Cell Signaling) and mouse anti-insulin (1:200; Abcam) antibodies. After incubation with fluorescently labeled anti-rabbit and anti-mouse secondary antibodies, the sections were viewed using an Olympus IX 70 fluorescence microscope.

Immunoblotting and Quantitative RT-PCR

Immunoblot and quantitative RT-PCR (RT-qPCR) assays were performed as previously described (13). Nuclear extraction from liver was performed using the Nuclear Extraction kit from Panomics according to the manufacturer's instructions. Total RNA was extracted from HCs using the RNeasy kit (Qiagen). cDNA was synthesized from 2 μg total RNA using oligo (dT) and Superscript II (Invitrogen).

G6pc Promoter-Luciferase Assay

WT mouse embryonic fibroblasts (MEFs) were transfected with a construct encoding nucleotides −1,227 to 57 of the human *G6pc* promoter fused to luciferase. MEFs were treated for 8 h with 0.15 mmol/L forskolin in serum-free medium prior to lysis and analysis of luciferase activity. Luciferase activity, measured in relative light units (RLU) per milligram of protein, was normalized to the untreated cells in each group.

Kinase Profiling

The protein kinases listed in Table 1 were tested against 10 μm cmpd 28 by Carna Biosciences using mobility shift assay or IMAP as described by the manufacturer, with the ATP concentration for each kinase adjusted for its Michaelis constant (K_m). Percent inhibition was calculated based on a 0% inhibition value (complete reaction mixture minus cmpd 28) and a 100% inhibition value (reaction mixture minus enzyme).

Statistical Analysis

All results are presented as mean ± SEM. *P* values were calculated using the Student *t* test for normally distributed

Table 1—Cmpd 28 selectively inhibits MK2 and MK3

Kinase	% inhibition by cmpd 28
AXL	5.3
JAK1	8.1
JAK2	5.6
JAK3	−6.2
MER	5.9
SRC	9.2
AMPKα1/β1/γ1	1.5
AMPKα2/β2/γ2	13.8
CK1γ1	−9.2
CK1γ2	−3.2
CK1γ3	−2.8
Erk1	1.2
Erk2	5.1
IKKα	4.8
IKKb	5.8
IKKe	−2.1
JNK1	−2.7
JNK2	6.5
JNK3	2.5
MAPKAPK2	98.6
MAPKAPK3	98.2
MAPKAPK5	59.2
p38α	3.8
p38β	4.7
p38γ	−3.1
p38δ	−5.6

The indicated protein kinases were screened against 10 μmol/L cmpd 28 using mobility shift assay or IMAP. AXL, Axl receptor tyrosine kinase; CK, Creatine kinase; Erk, extracellular signal–related kinase; IKK, I kappa B kinase; JAK, Janus kinase; MER, Mer tyrosine kinase; SRC, Proto-oncogene tyrosine-protein kinase Src.

data and the Mann-Whitney rank sum test for non–normally distributed data.

RESULTS

Cmpd 28 Is an Effective Inhibitor of MK2/3 Activity in Primary HCs and Inhibits Forskolin-Induced *G6pc* Expression

We first tested the ability of cmpd 28 to suppress MK2/3 activity in primary HCs by monitoring phosphorylation of the MK2/3 substrate, heat-shock protein (hsp)25 (16). For this purpose, we used tumor necrosis factor α as a potent stimulus of MK2/3 activation and found that cmpd 28 markedly decreased hsp25 phosphorylation (Supplementary Fig. 2*A*). We then turned our attention to HCs exposed to palmitate because palmitate mimics features of HC pathophysiology seen in obesity (21,22). Cmpd 28 effectively suppressed hsp25 phosphorylation in this model as well (Fig. 1*A*).

Our previous work showed that inhibition of hepatic p38 or MK2/3 by genetic targeting or dominant-negative constructs decreases glucagon-induced nuclear FoxO1 and thereby inhibits the expression of the gluconeogenic and glycogenolytic gene, glucose-6-phosphatase (*G6pc*) (13). We therefore asked whether cmpd 28 could suppress the ability of forskolin, which mimics glucagon by activating adenylate cyclase, to induce *G6pc* in primary HCs. We found that the drug potently suppressed both forskolin-induced hsp25 phosphorylation and *G6pc* expression,

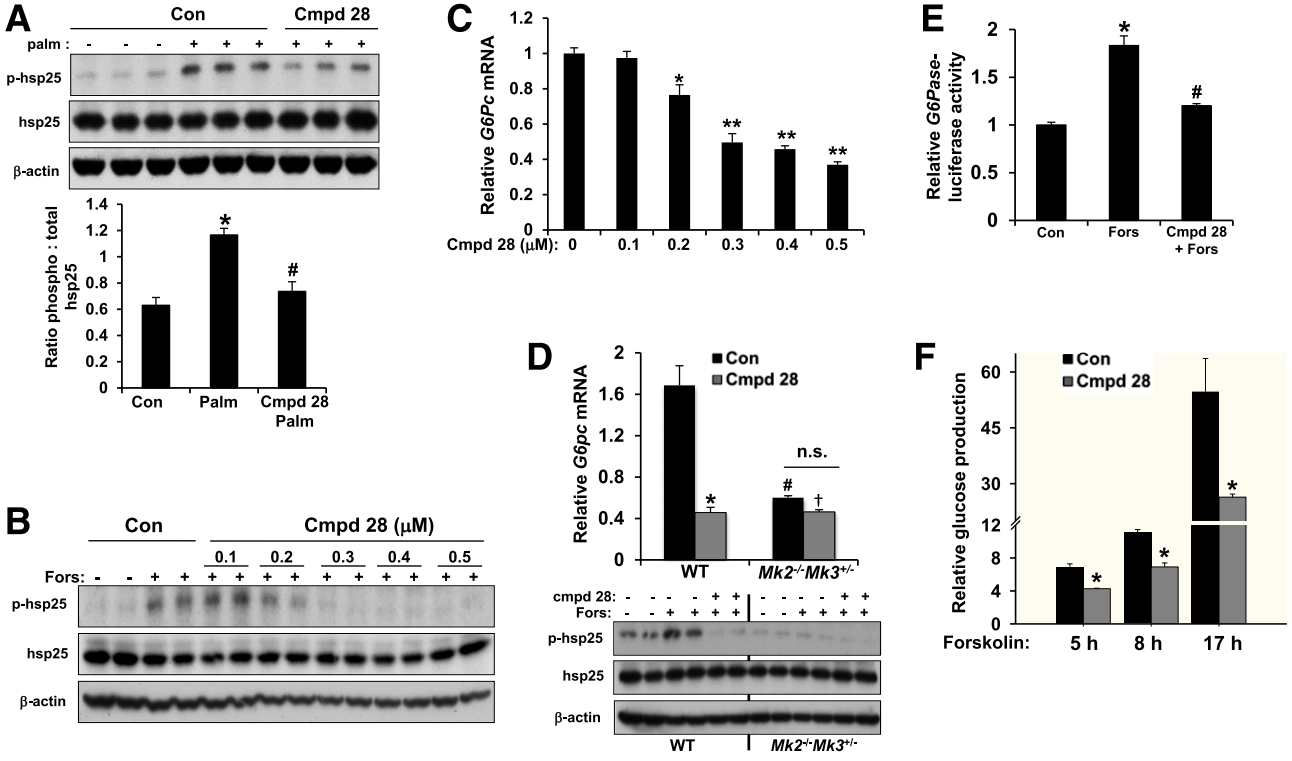

Figure 1—Cmpd 28 is an effective inhibitor of MK2/3 activity in liver cells and inhibits forskolin-induced hsp25 phosphorylation and *G6pc* expression. *A*: Primary HCs from WT mice were pretreated with either vehicle (Control [Con]) or 500 nm cmpd 28 for 1 h followed by incubation with either BSA control or 0.3 mmol/L palmitate (palm) for 6 h. Lysates were probed for p-hsp25, hsp25, and β-actin by immunoblot. Densitometric quantification of the immunoblot data are shown in the graph (differing symbols indicate $P < 0.05$) (mean ± SEM). p, phosphorylated; phospho, phosphorylated. *B*: Primary HCs from WT mice were pretreated with either vehicle (Con) or indicated concentrations of cmpd 28 for 1 h, followed by cotreatment with cmpd 28 with or without forskolin (Fors) for 1 h. Lysates were probed for p-hsp25, hsp25, and β-actin by immunoblot. p, phosphorylated *C*: Primary HCs from WT mice were serum depleted overnight and then pretreated with either vehicle (Con) or indicated concentrations of cmpd 28 for 1 h, followed by cotreatment with cmpd 28 with or without forskolin for 5 h. RNA was assayed for *G6pc* mRNA by RT-qPCR (*$P < 0.05$; **$P < 0.01$) (mean ± SEM). *D*: HCs from WT and $Mk2^{-/-}Mk3^{+/-}$ mice were serum depleted overnight and then pretreated with either vehicle (Con) or 500 nm cmpd 28 for 1 h, followed by cotreatment with cmpd 28 with or without forskolin for 5 h. RNA was assayed for *G6pc* mRNA by RT-qPCR (differing symbols indicate $P < 0.05$) (mean ± SEM). The protein lysates from a parallel set of cells were probed for p-hsp25, hsp25, and β-actin by immunoblot. n.s., nonsignificant; p, phosphorylated. *E*: WT MEFs were transfected with a luciferase fusion construct encoding nucleotides −1,227 to 57 of the *G6pc* promoter, which contains the FoxO1 binding sites of the promoter region. Relative luciferase activity was measured after pretreatment with vehicle (Con) or cmpd 28 for 1 h, followed by cotreatment with cmpd 28 with or without forskolin for 8 h (differing symbols indicate $P < 0.05$) (mean ± SEM). *F*: Primary HCs from WT mice were serum depleted overnight and then pretreated with either vehicle (Con) or 500 nm cmpd 28 for 1 h, followed by cotreatment with cmpd 28 and forskolin for the indicated times in serum- and glucose-free media. The glucose in the medium was assayed and normalized to total cell lysate (*$P < 0.05$) (mean ± SEM).

with a maximum effect at 500 nmol/L (Fig. 1*B* and *C*). To determine whether the mechanism was through MK2/3 inhibition, we conducted a parallel experiment comparing WT and $Mk2^{-/-}Mk3^{+/-}$ HCs (23). As expected, forskolin-induced p-hsp25 and *G6pc* mRNA induction were decreased in $Mk2^{-/-}Mk3^{+/-}$ vs. WT HCs, and the suppressive actions of cmpd 28 and MK2/3 deficiency were not additive (Fig. 1*D*). These data are consistent with the premise that cmpd 28 acts in the same pathway as MK2/3. As another assay, we used WT MEFs transfected with a luciferase fusion construct encoding the FoxO1 binding sites of the *G6pc* promoter (24,25), and we found that induction of luciferase through forskolin treatment was significantly blunted by cmpd 28 (Fig. 1*E*). Consistent with these data, cmpd 28 also inhibited forskolin-induced glucose production in primary HCs (Fig. 1*F*). Of note, cmpd 28 had no effect on cell viability under these conditions as determined by TUNEL assay (Supplementary Fig. 2*B*). We next profiled cmpd 28 for kinase selectivity by screening against a panel of 26 different protein kinases at a concentration of 10 μmol/L. As expected, cmpd 28 inhibited both MK2 and MK3, and it had no or little effect on the other kinases assayed (Table 1). Most importantly, cmpd 28 had no effect on CaMKII at the doses where it can efficiently inhibit forskolin-induced p-hsp25 (Supplementary Fig. 2*C*). These combined data show that cmpd 28 selectively inhibits MK2/3 and effectively lowers the expression of *G6pc*, which is consistent with the proposed mechanism of the drug's action, namely, inhibition of the CaMKII-MK2-FoxO1-*G6pc* pathway (13).

Cmpd 28 Treatment Improves Glucose Homeostasis in Obese Mice

To investigate the effect of MK2/3 inhibition on hepatic glucose metabolism in the setting of obesity, we treated *ob/ob* mice with injections of cmpd 28 (0.2 mg/kg body wt i.p.) or vehicle control. A dose range was estimated from in vitro potency data (19), and a pilot experiment showed that 8 days of daily treatment with 0.2 mg/kg body wt i.p. cmpd 28 effectively lowered fasting blood glucose in obese mice, whereas 0.02 mg/kg body wt had little effect, and no further effect was observed at 2 mg/kg body wt. Another pilot experiment showed that a single injection of 0.2 mg/kg body wt i.p. cmpd 28 led to peak plasma concentrations of ~45 ng/mL after 5 min, followed by significant levels of cmpd 28 accumulating in the liver, peaking at 15 min. The plasma half-life of cmpd 28 was ~1–2 h, and the liver half-life was ~2.75 h. After 3 weeks of once-daily i.p. injections of *ob/ob* mice with 0.2 mg/kg body wt cmpd 28, MK2/3 activity in the liver was inhibited as evidenced by reduced p-hsp25 levels (Fig. 2*A*). During the course of the treatment, cmpd 28 had no effect on body weight or food intake (Supplementary Fig. 3*A* and *B*), and plasma lipids showed a nonsignificant trend toward lower values (Supplementary Fig. 3*C*–*E*). Most importantly, cmpd 28 significantly lowered blood glucose and circulating plasma insulin levels of *ob/ob* mice as early as 3 days after treatment (Fig. 2*B* and *C*), and both end points remained lower during the 3-week course of the study (Fig. 2*D*–*F*). Drug treatment improved blood glucose response to glucose challenge and enhanced glucose disposal in response to insulin stimulation (Fig. 2*G* and *H*), which indicates an increase in insulin sensitivity. Drug-treated mice also displayed lower plasma glucose in response to pyruvate, which is a measure of hepatic glucose production (Fig. 2*I*). Cmpd 28 had similar effects in DIO mice; i.e., it lowered fasted and fed blood glucose and plasma insulin in the absence of any change in body weight (Fig. 3).

In order to assess whether the metabolic benefits of cmpd 28 in obese mice were due to its ability to inhibit MK2/3, we transduced *ob/ob* mice with adenoviral constructs encoding dominant-negative T222A-MK2 (DN-MK2) (26) or control LacZ and then treated the mice with cmpd 28 or vehicle for 7 days. We found that both dominant-negative MK2 and cmpd 28 treatment led to a decrease in blood glucose and plasma insulin (Fig. 4) in a manner that was not additive. These combined results demonstrate that MK2/3 suppression by either an allosteric inhibitor or a dominant-negative construct lowers blood glucose and improves insulin sensitivity in two models of obesity-induced insulin resistance.

We previously showed that genetic inhibition of the CaMKII-p38-MK2 pathway in the livers of obese mice has two beneficial actions: *1*) improvement of insulin-induced Akt phosphorylation by suppressing the endogenous Akt inhibitor Trb3 and *2*) suppression of gluconeogenic gene induction by decreasing nuclear FoxO1 (13,14). We therefore assessed the effect of cmpd 28 on these parameters in the livers of obese mice. Cmpd 28 treatment increased insulin-induced Akt activation and decreased the levels of Trb3, nuclear FoxO1, and mRNAs of three FoxO1-target genes: *G6pc*, *Pck1*, and *Igfbp1* (Fig. 5*A*–*C*). Drug treatment also increased insulin-induced Akt activation in skeletal muscle (Fig. 5*D*), which is consistent with an improvement in systemic glucose metabolism, whereas examination of islet morphology and function did not reveal significant effects after 2 weeks of treatment (Fig. 5*E*). These collective data support the conclusion that cmpd 28 improves metabolism in obese mice by blocking HGP and improving insulin signaling.

The Metabolic Improvement by Cmpd 28 and Metformin in Obese Mice Is Additive

Metformin is the most commonly used drug for non–insulin-dependent T2D (27). We therefore tested whether the beneficial metabolic effects of cmpd 28 would be additive with metformin by treating *ob/ob* mice with vehicle (control), metformin alone, cmpd 28 alone, or metformin plus cmpd 28. Metformin and cmpd 28 each decreased blood glucose, and, most importantly, the effect was additive (Fig. 6*A*). Similar results were obtained when the

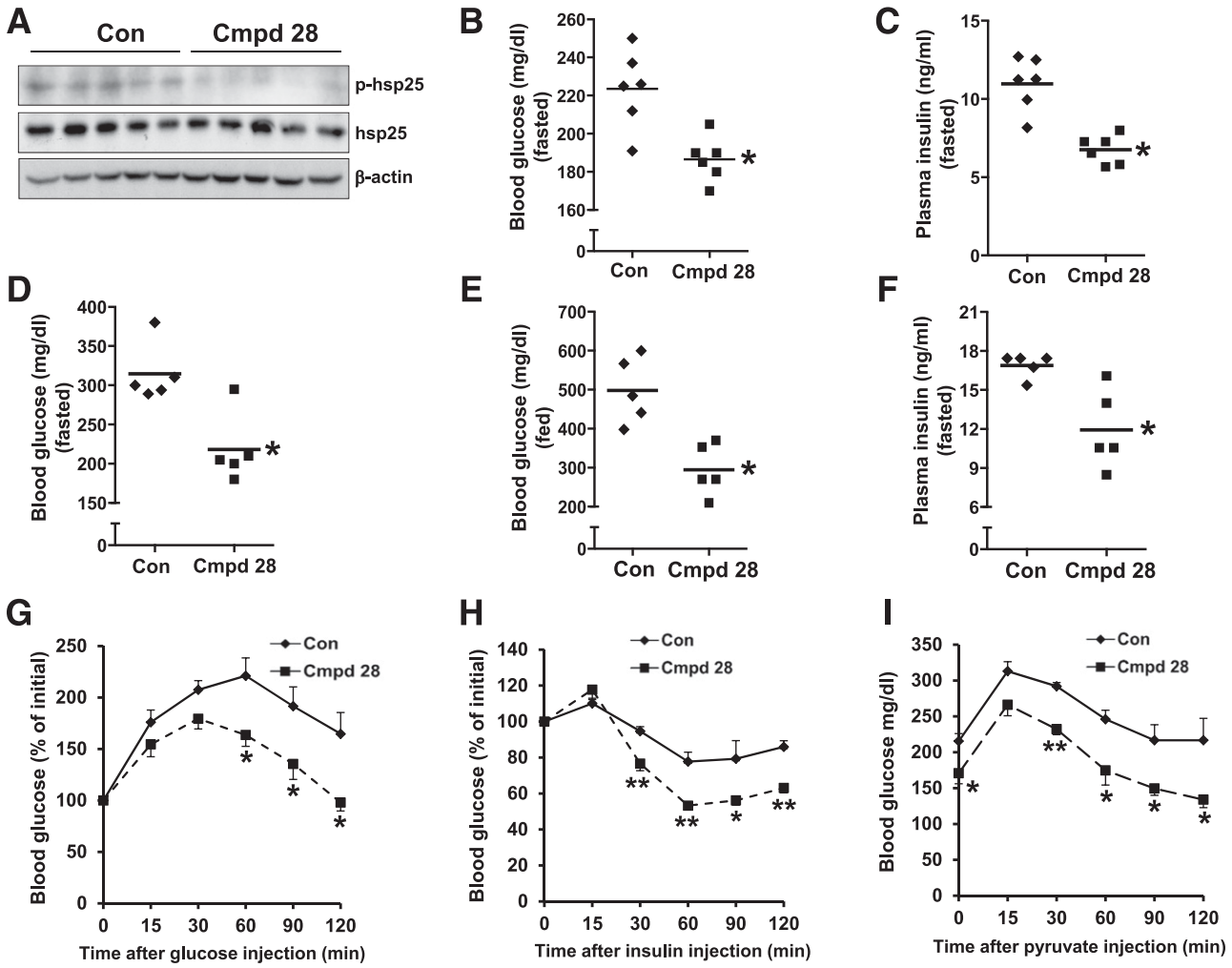

Figure 2—Cmpd 28 treatment improves glucose homeostasis in *ob/ob* mice. Ten-week-old *ob/ob* mice were injected with 0.2 mg/kg body wt i.p. cmpd 28 or vehicle (control [Con]) each day for 3 weeks (n = 5 mice per group). The mice were then assayed for hepatic p-hsp25, total hsp25, and β-actin by immunoblot (*A*). p, phosphorylated. *B* and *C*: Ten-week-old *ob/ob* mice were injected with 0.2 mg/kg body wt i.p. cmpd 28 or vehicle (Con) each day for 2 weeks (n = 6 mice per group). Blood glucose and plasma insulin levels after a 6-h fast at day 3 are shown (*$P < 0.05$) (mean ± SEM). *$P < 0.05$. *D–H*: The mice in *A* were assayed for the following parameters: 6-h fasting blood glucose levels at day 10 (*D*), fed blood glucose levels 1 h after drug administration at day 7 (*E*), 6-h fasting plasma insulin levels at day 10 (*F*), glucose tolerance test on day 8 (*G*), and insulin tolerance test on day 12 (*H*) (*$P < 0.05$; **$P < 0.01$) (mean ± SEM). *I*: The mice in *B* were assayed for blood glucose after a pyruvate challenge on day 9 (*$P < 0.05$; **$P < 0.01$) (mean ± SEM).

end point was suppression of plasma insulin as a measure of insulin sensitization (Fig. 6*B*). Moreover, there was also an additive effect on the lowering of hepatic *G6pc* mRNA (Fig. 6*C*). Note that neither treatment affected body weight in these mice (Fig. 6*D*). Thus, at the doses used in this experiment, cmpd 28 has additive beneficial metabolic effects with metformin in obese mice.

DISCUSSION

Obesity-induced T2D is a major health concern and a leading driver of cardiovascular disease, kidney failure, retinal disease, and other maladies in modern societies. The demand for new drugs is enormous as the prevalence of diabetes continues to grow worldwide. In particular, there is a critical need for safe and effective oral drugs that work in combination with the current leader, metformin, or that can be used in metformin-intolerant patients (28). Our recent work indicated that genetic-mediated suppression of the hepatic CaMKII-MK2 pathway safely improves both hyperglycemia and insulin resistance in mouse models of obesity. Here, we provide evidence that an allosteric MK2/3 inhibitor, cmpd 28, improves glucose homeostasis and insulin sensitivity in obese mice. Cmpd 28 and DN-MK2 were equally effective in lowering blood glucose and plasma insulin, and they did this in a nonadditive manner, suggesting an on-target mechanism of this MK2/3 inhibitor. Moreover, the mechanism of cmpd 28 differs from that of metformin and other T2D drugs, and cmpd 28 is additive with metformin in obese mice.

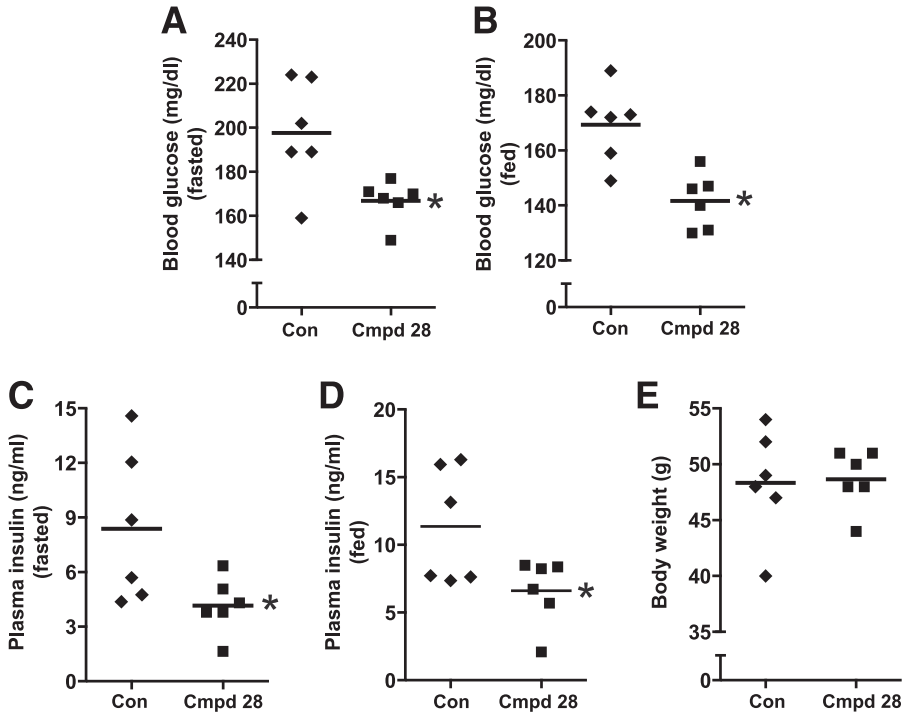

Figure 3—Cmpd 28 treatment improves glucose homeostasis in DIO mice. DIO mice (17 weeks old) were injected with 0.2 mg/kg body wt i.p. cmpd 28 or vehicle (control [Con]) each day for 3 weeks (n = 6 mice per group). The mice were then assayed for fasting blood glucose (*A*), fed blood glucose (*B*), fasting plasma insulin (*C*), and fed plasma insulin (*D*), and body weight was determined (*E*) (*$P < 0.05$) (mean ± SEM).

Preclinical and clinical studies with p38 inhibitors have shown that they are hepatotoxic, which is related to a p38-mediated feedback loop involving TGFβ-activated kinase 1 (TAK1) and c-Jun N-terminal kinase (JNK) activation (29). This feedback loop is not activated by complete MK2/3 deficiency or MK2 inhibitors (16). Moreover, whereas p38α knockout mice are embryonic lethal (30), mice totally lacking both MK2 and MK3 ($Mk2^{-/-}Mk3^{-/-}$) show no overt adverse effects (20). They are protected from septic shock; inflammatory, ischemic, neurodegenerative diseases; and certain types of cancer. Importantly, hypercholesterolemic $Mk2^{-/-}$ mice on an $Ldlr^{-/-}$ background had lower atherosclerotic lesion development, indicating a beneficial effect of MK2 inhibition on atherosclerosis development (31). In addition, MK2 inhibitors are being investigated for their anti-inflammatory and possible antitumor properties (32). Finally, MK2 plays a pathological role in heart failure, suggesting a possible beneficial effect of MK2/3 inhibitors for this T2D-driven disease as well (26).

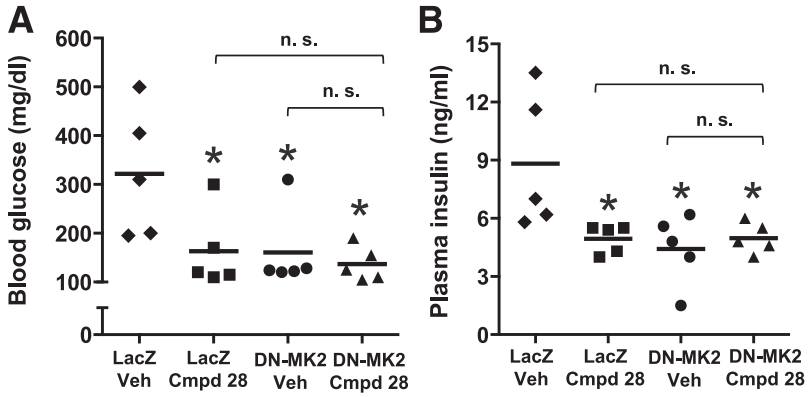

Figure 4—The metabolic improvement by cmpd 28 and dominant-negative MK2 in obese mice is not additive. Ten-week-old *ob/ob* mice were transduced with adeno-LacZ or adeno–T222A-MK2 (dominant negative), which inhibits hepatic MK2. Mice were then treated with 0.2 mg/kg body wt i.p. cmpd 28 or vehicle (Veh) for 7 days (n = 5 mice per group). After a 6-h fast, the mice were assayed for fasting blood glucose (*A*) and plasma insulin (*B*) (*$P < 0.05$) (mean ± SEM). n.s., nonsignificant.

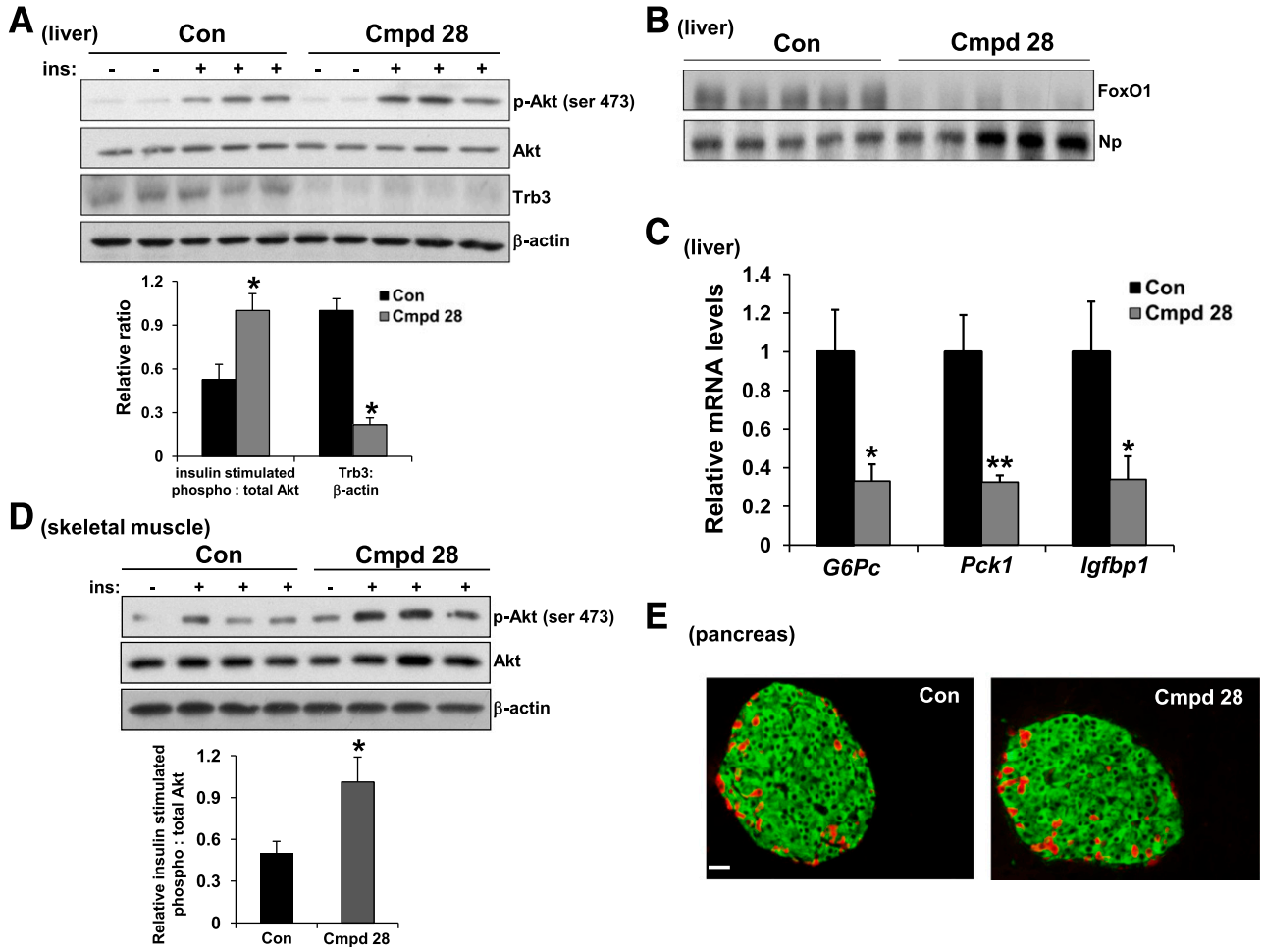

Figure 5—Cmpd 28 treatment improves insulin-induced Akt phosphorylation and lowers the expression of gluconeogenic genes in obese mice. Ten-week-old *ob/ob* mice were injected with 0.2 mg/kg body wt i.p. cmpd 28 or vehicle (control [Con]) each day for 3 weeks (n = 5 mice per group). *A*: The mice were fasted for 6 h and then injected with 2 IU/kg body wt insulin (ins) through the portal vein. After 3 min, livers were harvested, and total liver extracts were assayed for p-Akt, Akt, Trb3, and β-actin by immunoblot. Densitometric quantification of the immunoblot data is shown in the graph (*P < 0.05) (mean ± SEM). *B*: Nuclear protein isolated from the mice in *A* was probed for FoxO1 and nucleophosmin (Np) by immunoblot. *C*: RNA was extracted from liver and assayed by RT-qPCR for *G6pc*, *Pck1*, and *Igfbp1* mRNA (*P < 0.05; **P < 0.01) (mean ± SEM). *D*: Seventeen-week-old DIO mice were injected with 0.2 mg/kg body wt i.p. cmpd 28 or vehicle (Con) each day for 3 weeks. The mice were fasted for 5 h and then injected with 1 IU/kg body wt insulin (ins) through the portal vein. After 4 min, skeletal muscle was harvested, and total skeletal muscle extracts were assayed for p-Akt, Akt, and β-actin by immunoblot. Densitometric quantification of the immunoblot data is shown in the graph (*P < 0.05) (mean ± SEM). *E*: Pancreatic islets from *ob/ob* mice treated with 0.2 mg/kg body wt i.p. cmpd 28 or vehicle (Con) each day for 2 weeks were immunostained for insulin (green) and glucagon (red). p, phosphorylated; phospho, phosphorylated.

Despite the possibility of multiple beneficial effects of MK2/3 inhibition, drug development in the T2D area would focus on partial suppression of MK2/3 activity in the liver, which was the case for cmpd 28 based on the p-hsp25 and pharmacokinetic data. Interestingly, complete germline deletion of MK2 in all tissues was recently reported to worsen metabolism in mice, which was attributed to proinflammatory polarization of adipose tissue macrophages and decreased expression of the glucose transporter GLUT4 (33). Whether these effects were secondary to compensatory changes in response to complete germline deletion of MK2 or other mechanisms remains to be investigated, but we found no M1 polarization of adipose tissue macrophages or reduction in adipose tissue GLUT4 levels in mice treated with the MK2/3 inhibitor, cmpd 28, compared with controls (Supplementary Fig. 4).

Mice completely lacking MK2 are also more susceptible to a high (but not lower) inoculum of *Listeria monocytogenes* compared with WT mice, but they otherwise show a remarkably intact host defense mechanism, including resistance to endotoxic shock (34). In this light, we recently discovered that MK2 inhibition promotes an inflammatory resolution response (35), and responses of this nature can actually bolster host defense (36,37).

As mentioned above, diabetes in obese humans and mice is known to be exacerbated by excess glucagon action at the level of the HC, and attempts to lower glucagon

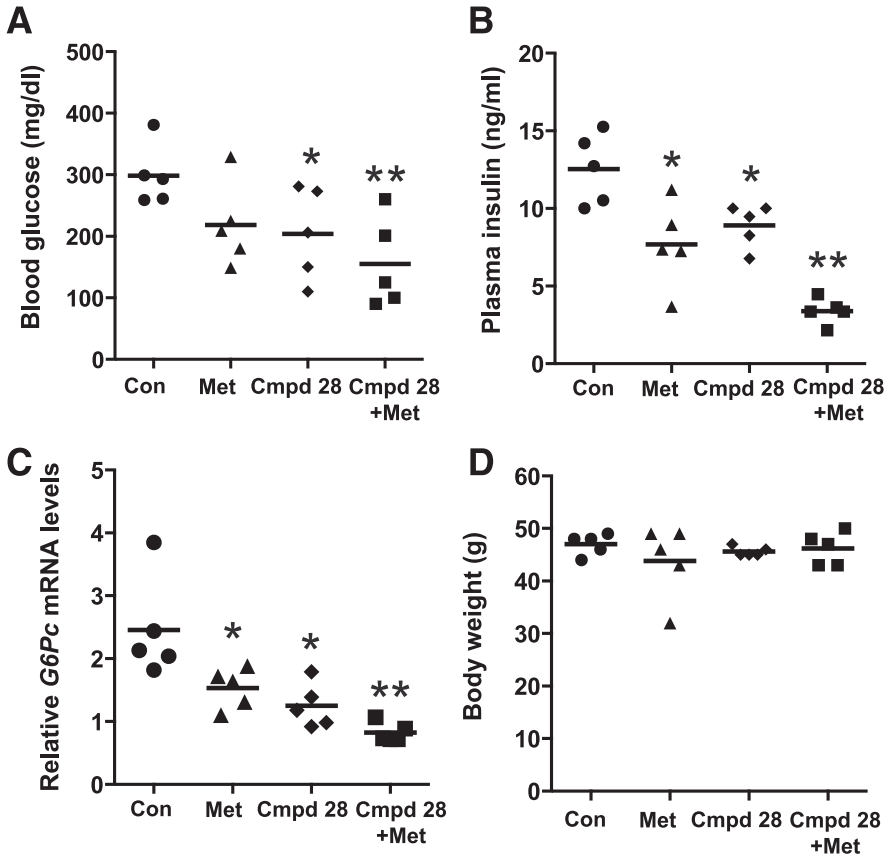

Figure 6—The metabolic improvement by cmpd 28 and metformin in obese mice is additive. Ten-week-old *ob/ob* mice were treated intraperitoneally with vehicle (control [Con]), 200 mg/kg body wt metformin (Met), 0.2 mg/kg body wt cmpd 28, or both compounds for 14 days (n = 5 mice per group). The mice were assayed for fasting blood glucose (*A*), plasma insulin (*B*), hepatic *G6pc* mRNA expression levels (*C*), and body weight (*D*) (*$P < 0.05$; **$P < 0.01$) (mean ± SEM).

action using glucagon receptor antagonists (GRAs) have recently gained extensive interest (38–40). GRAs effectively lower blood glucose in humans with T2D, but GRAs increase plasma LDL (11,41,42), which has presented a significant block to their development as T2D drugs. Interestingly, cmpd 28 does not raise blood lipids and even shows a trend toward lowering them. Future studies will be required to further validate this point, i.e., through direct comparison of GRAs and allosteric MK2/3 inhibitors, and to elucidate the mechanism. Indeed, although mice with small interfering RNA–mediated blockade of the glucagon receptor demonstrated increased hepatic lipid synthesis (11), the mechanism of the lipid-raising effect of GRAs in humans is not known. In theory, it is possible that MK2/3 inhibitors, by targeting a downstream node of glucagon receptor signaling, avoid the hyperlipidemic effect of GRAs or that MK2/3 inhibitors have an additional effect that neutralizes the lipid-raising effects of GR pathway inhibition. The importance of this issue is related to the increased risk of cardiovascular disease in patients with T2D, leading the FDA to require clinical trials to assess the cardiovascular safety of all new T2D drugs. The potential protective effects of MK2/3 inhibition on atherosclerosis and heart failure (above) may indicate that cardiovascular safety may not be an issue with MK2/3 inhibitors and may even represent an additional benefit of this class of drugs.

Funding. This work was supported by American Heart Association Scientist Development grant (11SDG5300022) and New York Obesity Nutrition Research Center Pilot and Feasibility grant (DK26687) to L.O., Deutsche Forschungsgemeinschaft (SFB 566 B12) to M.G., and National Institutes of Health grants HL087123 and HL075662 to I.T. Cmpd 28 synthesis was performed by the chemists at the Organic Chemistry Collaborative Center of Columbia University and supported by the New York Stem Cell Program (contract no. C0267152) and the National Center for Advancing Translational Sciences, National Institutes of Health (UL1 TR000040).

Duality of Interest. L.O., B.H., M.H.S.-W., and I.T. are in the group of cofounders of Tabomedex Biosciences, LLC, which is developing inhibitors for the treatment of type 2 diabetes. No other potential conflicts of interest relevant to this article were reported.

Author Contributions. L.O. and I.T. designed research. L.O., X.X., S.-X.D., D.S.G., and T.T. performed research. S.C., M.G., and D.W.L. contributed new reagents/analytic tools. L.O., X.X., S.-X.D., D.S.G., T.T., S.C., B.H., M.H.S.-W., D.W.L., and I.T. analyzed data. L.O., M.G., and I.T. wrote the manuscript. L.O. is the guarantor of this work and, as such, had full access to all the data in the study and takes responsibility for the integrity of the data and the accuracy of the data analysis.

References

1. Kuritzky L, Samraj GP. Enhanced glycemic control with combination therapy for type 2 diabetes in primary care. Diabetes Ther 2011;2:162–177
2. Lin HV, Accili D. Hormonal regulation of hepatic glucose production in health and disease. Cell Metab 2011;14:9–19
3. Unger RH, Cherrington AD. Glucagonocentric restructuring of diabetes: a pathophysiologic and therapeutic makeover. J Clin Invest 2012;122:4–12
4. D'Alessio D. The role of dysregulated glucagon secretion in type 2 diabetes. Diabetes Obes Metab 2011;13(Suppl. 1):126–132
5. Ozcan U, Cao Q, Yilmaz E, et al. Endoplasmic reticulum stress links obesity, insulin action, and type 2 diabetes. Science 2004;306:457–461
6. Gregor MF, Yang L, Fabbrini E, et al. Endoplasmic reticulum stress is reduced in tissues of obese subjects after weight loss. Diabetes 2009;58:693–700
7. Fu S, Yang L, Li P, et al. Aberrant lipid metabolism disrupts calcium homeostasis causing liver endoplasmic reticulum stress in obesity. Nature 2011; 473:528–531
8. Park SW, Zhou Y, Lee J, Lee J, Ozcan U. Sarco(endo)plasmic reticulum Ca2+−ATPase 2b is a major regulator of endoplasmic reticulum stress and glucose homeostasis in obesity. Proc Natl Acad Sci U S A 2010; 107:19320–19325
9. Mu J, Qureshi SA, Brady EJ, et al. Anti-diabetic efficacy and impact on amino acid metabolism of GRA1, a novel small-molecule glucagon receptor antagonist. PLoS ONE 2012;7:e49572
10. Sloop KW, Cao JX, Siesky AM, et al. Hepatic and glucagon-like peptide-1-mediated reversal of diabetes by glucagon receptor antisense oligonucleotide inhibitors. J Clin Invest 2004;113:1571–1581
11. Han S, Akiyama TE, Previs SF, et al. Effects of small interfering RNA-mediated hepatic glucagon receptor inhibition on lipid metabolism in db/db mice. J Lipid Res 2013;54:2615–2622
12. Ozcan U, Yilmaz E, Ozcan L, et al. Chemical chaperones reduce ER stress and restore glucose homeostasis in a mouse model of type 2 diabetes. Science 2006;313:1137–1140
13. Ozcan L, Wong CC, Li G, et al. Calcium signaling through CaMKII regulates hepatic glucose production in fasting and obesity. Cell Metab 2012;15:739–751
14. Ozcan L, Cristina de Souza J, Harari AA, Backs J, Olson EN, Tabas I. Activation of calcium/calmodulin-dependent protein kinase II in obesity mediates suppression of hepatic insulin signaling. Cell Metab 2013;18:803–815
15. Dulos J, Wijnands FP, van den Hurk-van Alebeek JA, et al. p38 inhibition and not MK2 inhibition enhances the secretion of chemokines from TNF-α activated rheumatoid arthritis fibroblast-like synoviocytes. Clin Exp Rheumatol 2013;31:515–525
16. Ronkina N, Menon MB, Schwermann J, et al. MAPKAP kinases MK2 and MK3 in inflammation: complex regulation of TNF biosynthesis via expression and phosphorylation of tristetraprolin. Biochem Pharmacol 2010;80:1915–1920
17. Heinrichsdorff J, Luedde T, Perdiguero E, Nebreda AR, Pasparakis M. p38 alpha MAPK inhibits JNK activation and collaborates with IkappaB kinase 2 to prevent endotoxin-induced liver failure. EMBO Rep 2008;9:1048–1054
18. Hui L, Bakiri L, Mairhorfer A, et al. p38alpha suppresses normal and cancer cell proliferation by antagonizing the JNK-c-Jun pathway. Nat Genet 2007;39: 741–749
19. Huang X, Zhu X, Chen X, et al. A three-step protocol for lead optimization: quick identification of key conformational features and functional groups in the SAR studies of non-ATP competitive MK2 (MAPKAPK2) inhibitors. Bioorg Med Chem Lett 2012;22:65–70
20. Ronkina N, Kotlyarov A, Dittrich-Breiholz O, et al. The mitogen-activated protein kinase (MAPK)-activated protein kinases MK2 and MK3 cooperate in stimulation of tumor necrosis factor biosynthesis and stabilization of p38 MAPK. Mol Cell Biol 2007;27:170–181
21. Boden G, She P, Mozzoli M, et al. Free fatty acids produce insulin resistance and activate the proinflammatory nuclear factor-kappaB pathway in rat liver. Diabetes 2005;54:3458–3465
22. Achard CS, Laybutt DR. Lipid-induced endoplasmic reticulum stress in liver cells results in two distinct outcomes: adaptation with enhanced insulin signaling or insulin resistance. Endocrinology 2012;153:2164–2177
23. Gaestel M. MAPKAP kinases - MKs - two's company, three's a crowd. Nat Rev Mol Cell Biol 2006;7:120–130
24. Ayala JE, Streeper RS, Desgrosellier JS, et al. Conservation of an insulin response unit between mouse and human glucose-6-phosphatase catalytic subunit gene promoters: transcription factor FKHR binds the insulin response sequence. Diabetes 1999;48:1885–1889
25. von Groote-Bidlingmaier F, Schmoll D, Orth HM, Joost HG, Becker W, Barthel A. DYRK1 is a co-activator of FKHR (FOXO1a)-dependent glucose-6-phosphatase gene expression. Biochem Biophys Res Commun 2003;300: 764–769
26. Streicher JM, Ren S, Herschman H, Wang Y. MAPK-activated protein kinase-2 in cardiac hypertrophy and cyclooxygenase-2 regulation in heart. Circ Res 2010;106:1434–1443
27. Hundal RS, Krssak M, Dufour S, et al. Mechanism by which metformin reduces glucose production in type 2 diabetes. Diabetes 2000;49:2063–2069
28. What comes after metformin for type 2 diabetes? Med Lett Drugs Ther 2012;54:58–59
29. Cheung PC, Campbell DG, Nebreda AR, Cohen P. Feedback control of the protein kinase TAK1 by SAPK2a/p38alpha. EMBO J 2003;22:5793–5805
30. Adams RH, Porras A, Alonso G, et al. Essential role of p38alpha MAP kinase in placental but not embryonic cardiovascular development. Mol Cell 2000;6: 109–116
31. Jagavelu K, Tietge UJ, Gaestel M, Drexler H, Schieffer B, Bavendiek U. Systemic deficiency of the MAP kinase-activated protein kinase 2 reduces atherosclerosis in hypercholesterolemic mice. Circ Res 2007;101:1104–1112
32. Duraisamy S, Bajpai M, Bughani U, Dastidar SG, Ray A, Chopra P. MK2: a novel molecular target for anti-inflammatory therapy. Expert Opin Ther Targets 2008;12:921–936
33. de Boer JF, Dikkers A, Jurdzinski A, et al. Mitogen-activated protein kinase-activated protein kinase 2 deficiency reduces insulin sensitivity in high-fat diet-fed mice. PLoS ONE 2014;9:e106300
34. Lehner MD, Schwoebel F, Kotlyarov A, Leist M, Gaestel M, Hartung T. Mitogen-activated protein kinase-activated protein kinase 2-deficient mice show increased susceptibility to Listeria monocytogenes infection. J Immunol 2002; 168:4667–4673
35. Fredman G, Ozcan L, Spolitu S, et al. Resolvin D1 limits 5-lipoxygenase nuclear localization and leukotriene B4 synthesis by inhibiting a calcium-activated kinase pathway. Proc Natl Acad Sci U S A 2014;111:14530–14535
36. Serhan CN. Pro-resolving lipid mediators are leads for resolution physiology. Nature 2014;510:92–101
37. Tabas I, Glass CK. Anti-inflammatory therapy in chronic disease: challenges and opportunities. Science 2013;339:166–172
38. DeMong D, Dai X, Hwa J, et al. The discovery of N-((2H-tetrazol-5-yl)methyl)-4-((R)-1-((5r,8R)-8-(tert-butyl)-3-(3,5-dichlorophenyl)-2-oxo-1,4-diazaspiro[4.5]dec-3-en-1-yl)-4,4-dimethylpentyl)benzamide (SCH 900822): a potent and selective glucagon receptor antagonist. J Med Chem 2014;57:2601–2610
39. Xiong Y, Guo J, Candelore MR, et al. Discovery of a novel glucagon receptor antagonist N-[(4-(1S)-1-[3-(3, 5-dichlorophenyl)-5-(6-methoxynaphthalen-2-yl)-1H-pyrazol-1-yl]ethylphenyl)carbonyl]-β-alanine (MK-0893) for the treatment of type II diabetes. J Med Chem 2012;55:6137–6148
40. Qureshi SA, Rios Candelore M, Xie D, et al. A novel glucagon receptor antagonist inhibits glucagon-mediated biological effects. Diabetes 2004;53: 3267–3273
41. Gelling RW, Du XQ, Dichmann DS, et al. Lower blood glucose, hyperglucagonemia, and pancreatic alpha cell hyperplasia in glucagon receptor knockout mice. Proc Natl Acad Sci U S A 2003;100:1438–1443
42. Longuet C, Sinclair EM, Maida A, et al. The glucagon receptor is required for the adaptive metabolic response to fasting. Cell Metab 2008;8:359–371